Recruitment, development and mortality of Calanus finmarchicus in the Georges Bank region

Xingwen Li[1],Dennis J. McGillicuddy[1], Jr., Edward G. Durbin[2]

[1] Applied Ocean Physics and Engineering Department, Woods Hole Oceanographic Institution, Woods Hole, MA 02543, USA
[2] Graduate School of Oceanography, University of Rhode Island, South Ferry Rd, Narragansett, Rhode Island 02282, USA

Abstract

An adjoint data assimilation approach was used to quantify the time-space-stage specified physical and biological controls on *Calanus finmarchicus* N_3 to C_6 stages over Georges Bank and its surrounding regions. Large seasonal and spatial variabilities are present in the inferred supply sources, mortality rates, computed molting fluxes and physical transports. Partially recovered off-bank initial conditions show that the deep basins in the Gulf of Maine, and the Scotian Shelf are major offbank source regions of early stage nauplii, C_5 and C_6 in January. In the growing season from January to April, inferred sources of young nauplii N_3 are mainly confined on Georges Bank, especially on the Northeast Peak. These on-bank sources of young nauplii N_3 are able to populate the bank with nauplii in late winter, becoming copepodites in spring. Large mortality rates of stages N_4 - C_2 between January - February are the main regulators to limit the population increase rates. In the meantime, advection and mixing processes transport this species from source regions on Georges Bank to surrounding waters in the Gulf of Maine, the continental slope and South Atlantic Bight. Between April - May, the population dynamics on the bank are driven by molting from lower to higher stages. Between May - June, abundances of copepodites drop sharply on Georges Bank, especially on the Crest. Large mortality rates are mainly responsible for the population decline. In addition, down-stream transport of advection and down-gradient transport of turbulent mixing enforce the June decline. Mortality rates of N_4 to C_2 are large between January -March and May - June. Mortality rates of C_5 and C_6 are large between April - June. *Calanus finmarchicus* are most vulnerable to death at stages N_6 and C_1, but most unlikely to die at stages C_3 and C_4. When they mature to adults, their mortality rates are large in the warm water of early summer.

Objective

—to infer and interpret the first order inferences of the population dynamics of *Calanus finmarchicus* species, by combining a multi-stage physical-biological model with the observations, i.e., the mean seasonal cycle of vertically-integrated distributions (Figure 1) of N_3 to C_6 stages from 5 years of GLOBEC observations.

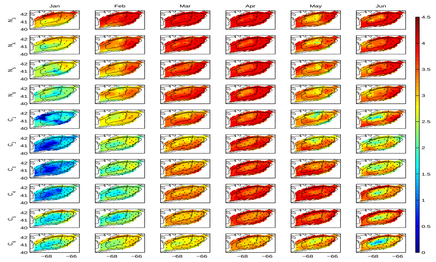

Figure 1 Observed climatological distributions of vertically-integrated abundances ($\log_{10}(1+\#/m^2)$) of *Calanus finmarchicus* N_3 - C_6 between 1995 - 1999. Black dots represent observational stations.

Model description

forward model:

—2D vertically-averaged off-line version of a finite element hydrodynamic model (Lynch et al., 1996).
— bimonthly climatology physical environment.

$$\frac{\partial C_i}{\partial t} + \vec{\mathbf{v}} \cdot \nabla C_i - \frac{1}{H}\nabla \cdot (HK\nabla C_i) = \delta_{i-1}R - F_i + (F_{i-1} + \mu_i C_i)(1 - \delta_{i-1}). \quad (1)$$

C — vertically-averaged zooplankton concentration.
R — input sources and mortality of N_3;
δ_{i-1} = 1 at i=1 and zero at other stages;
μ_i– mortality with negative values.
$F_i = \frac{C_i}{D_i}$, with the stage duration D_i stage-specified, temperature and food dependent (Campbell et al., 2001).

The **adjoint method** is used to minimize the model-data misfit (accumulated between Jan-Jun).
Cost function J,

$$J = \frac{1}{N_{mon}} \sum_{k}^{N_{mon}} \frac{1}{N_{stage}} \sum_{j}^{N_{stage}} \frac{1}{N_{obs}} \sum_{i}^{N_{obs}} (C_m - C_{obs})^2. \quad (2)$$

Control variables: monthly varying R, μ_i over the whole model domain, and the off-bank initial fields. All control variables are allowed to vary independently at corresponding model nodes. The first guess of those control variables are all set to zero.
A quasi-Newton algorithm for solving large nonlinear optimization with simple bounds (Byrd et al., 1995) is used to minimize the cost function.

Results

The constrained model successfully reproduces the most salient features of the observations. **Partially recovered offbank initial conditions**: By middle January, GB and its surrounding regions of the GOM and the Scotian Shelf have already been populated with young nauplii. Moderate abundances of C_4 - C_6 also appear there.

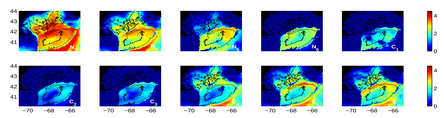

Figure 2 Optimal initial fields. The first estimates of initial values outside the data area (white area in Figure 1) are zeros.

Inferred sources/sinks R:
JF–the strongest on Northeast Peak and the Crest.
FA–Sources are strong on Northeast Peak; mortality appear on the SF.
AM–small.
MJ–becomes strong again along the bank periphery.

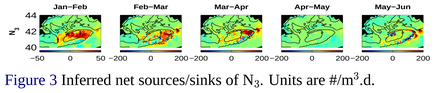

Figure 3 Inferred net sources/sinks of N_3. Units are #/m^3.d.

The **computed molting fluxes** reveal the subsequent development of *C.f.* stages. The development of nauplii begins as early as January; substantial development of copepodites starts in March.

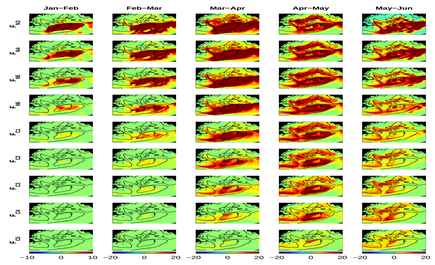

Figure 4 Computed monthly mean molting fluxes. Units are #/m^3.d

Inferred mortality: located mostly near GB
Distributions of C.f. mortality rates are similar within three groups: (I) N_4 - C_2, (II) C_3 and C_4, (III) C_5 and C_6.
Large seasonal variability
The peak mortality seasons of group I appear between January - March and May - June. Mortality rates of group II are very small. For group III, their mortality rates are large between April - June.

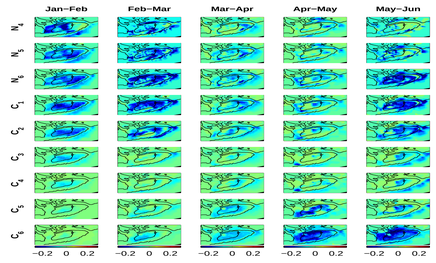

Figure 5: The inferred mortality rates. Units are d^{-1}.

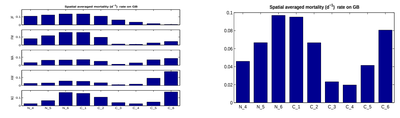

Figure 6 The spatially averaged mortality rates (presented in absolute values) on GB. Left panel:mean values between Jan. - Jun.

Recruitment: By mid-January, C_6 abundance is relatively high along the Northern Flank. The adults are then transported clockwise to the Northeast Peak and the Crest, by the modeled circulation. High reproduction rates at young stages exceed their large mortality rates, and quickly populate GB with nauplii. The young nauplii on GB are then transported either down-stream to the South Atlantic Bight or to the ambient GOM and Slope Water, and molt to higher stages.

Disappearance Large mortality rates are mainly responsible for the population decrease between MJ. The negative differences between the input and output molting fluxes also contribute to the C_3 and C_4 decrease. In addition, wash away effect of advection, and down-gradient transport of turbulent mixing reinforce the June decline.

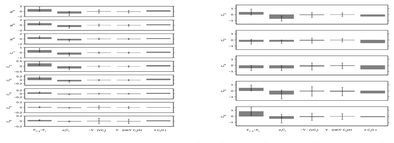

Figure 7 Space-time averaged values of controls on GB between JF (left) and MJ (right). The values are presented on a log scale $A/|A| \times log_{10}[(1 + abs(A))$, where A represents the values of the controls. Units are $log_{10}(1 + \#/m^3.d)$. Error bars present standard deviation of the spatial averages of the monthly means. Note that the scales of panels are different

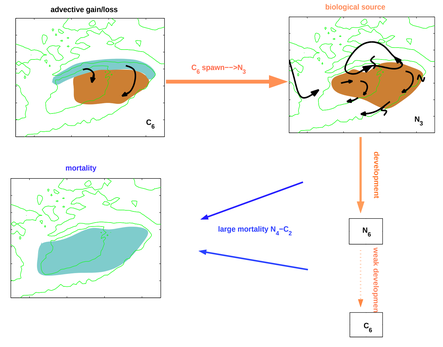

Figure 8 Schematic cartoon of *C.f.* population dynamics near GB between January - February. Biological sources and advective gains are represented by brown color; mortality and advective losses are represented by blue color. Arrows represent advection and curved lines represent mixing processes.

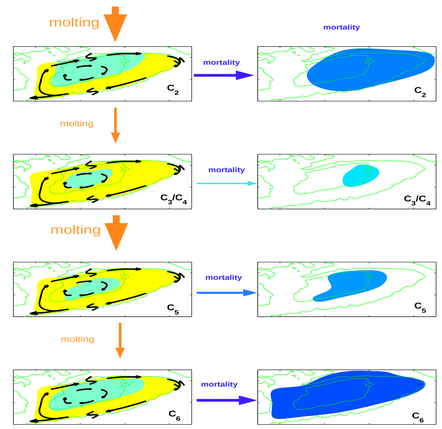

Figure 9 Inferred mechanisms leading to the disappearance of *C.f.* stages C_2 - C_6 from the Crest in June. The abundances (left panels) in green color are low; those in yellow are relatively high. Mortality is represented in blue. Arrows represent advection and curved lines represent mixing processes.

Acknowledgments

This work was supported by US GLOEBC-01: Integration and Synthesis of Georges Bank Broad-Scale Survey Results (NSF, NOAA)

References

[1] Byrd, R. H., P. Lu and J. Nocedal, 1995. A limited memory algorithm for bound constrained optimization. SIAM Journal on Scientific and Statistical Computing, 16, 1190-1208.

[2] Campbell, R. G., M. M. Wagner, G. J. Teegarden, C. A. Boudreau, and E. G. Durbin, 2001. Growth and development rates of the copepod *C.f.* reared in the laboratory. Mar. Ecol. Prog. Ser. 221, 161-183.

[3] Lynch, D. R., J. T. C. IP, C. E. Naimie, and F. E. Werner, 1996. Comprehensive coastal circulation model with application to the Gulf of Maine. Continental Shelf Research, 16, 875-906.